Analysis of Optical Frequency Locked Loop (OFLL) For Laser Communications Using Finite Response-Time Cavity Model

bloc Z. Win and Randy Bartman

Jet Propulsion Laboratory, California Institute of Technology

4800 Oak Grove Drive, Pasadena, California, USA

Abstract

Frequency stabilization plays a very critical role in diverse applications such as long distance fiber and free space optical communications, interferometric sensing, optical gyroscopes, squeezed states of light, atomic beam trapping, and gravity wave detection,

Frequency stabilization can be achieved by locking lasers to a Fabry-Perot etalon. One possible frequency stabilization technique is to use an oscillator that dithers o: modulates the frequency of the lasers, The frequency-clithtmd laser light is analyzed via transmission through the Fabry-Perot. The output of the etalon is detected by a photodetector and then correlated wit h the dithering oscillator signal to obtain frequency locking error estimates and subsequently control the frequency of the lasers.

A theoretical analysis is performed for a Fabry-Perot frequency stabilization subsystem, disturbed by shot noise and frequency noise consisting of white, 1/~, and $1/f^2$ components. Contributions of the shot noise and frequency noise components to the tot al frequency locking error variance are derived. Given the characteristics of the etalon, an optimal depth of frequency modulation is calculated for the dithering oscillator that maximizes the locking error signal amplitude and hence results in the best possible locking performance. Total frequency locking error as a function of loop bandwidth is displayed.

Finally, the expected performance of an optimized Fabry-1'trot stabilization system is estimated.

I. Introduction

Frequency stabilization plays a very critical roles in applications such as data communication, Doppler tracking, and ultra-high precision absolute-distal]ce measuring, where coherent optical heterodyne detection is utilized. The requirement of the laser frequency stability for coherent optical communications was investigated in [1], and shown that the required signal power for, phase locked receiver can be further reduced provided that transmit and local oscillator laser are stabilized to a external reference. Further more, optical carrier capable of achieving similar frequency stability to current-day RF system can potentially offer significant improvement in space-craft navigation capabilities [1].

Optimal loop bandwidth of the optical phase-locked loop decreases with decreasing signal-to-noise ratio [2], ant] therefore excellent frequency stability is required in order to achieve phase coherent optical heterodyne reception when low signal power reception is expected. Since the spectral filtering is performed at intermediate frequency, where the bandwidth selection is very effective, heterodyne detection offers a good background noise reject ion, Band width select ive nat ure of coherent receiver can also lead to a more efficient usc of the optical spectrum and potential for multiple access communication. Similarly in high-precision metrology using multiple-wavelengt h interferomet ry, high] y st able laser sources are required to achieve sub- nanomet er measurements of absolute. dist antes [3, 4]. In all such applications, frequency of the lasers must be stabilized, at frequencies with relative offsets to each other, over prolonged period of time. This can be achieved by locking the lasers to different order peaks of a single Fabry-Perot etalon (FPE) as described below.

The conceptual design of an FPE two-laser frequency stabilization system is shown in Fig. 1. The two laser stabilization systems arc essentially independent and they share the

single FPE and single drive oscillator on a non-interacting basis. Whether or not one laser is locked to the FPE makes no difference to the other laser, and hence only one system will be discussed in the following.

The laser frequency is modulated, at a rate much higher than the basic laser frequency jitter, using the signal from the common drive oscillator. After passing through the FPE, the frequency-dithered laser signal is registered by a photodetector, If the laser's frequency is accurately locked to the assigned FPE transmission peak, the component of the photodetector output at the fundamental oscillator frequency will be zero, However, a small offset between the laser frequency and the transmission peak of the FPE will result in a non-zero output at the fundamental frequency. The photodetector output is homodyned with drive oscillator signal to derive an estimate of the laser-vs.-FPll frequency offset. The resulting error signal is low-pass filtered and fed hack to the control inputs of the laser to effect a frequency correction, A schematic of this optical frequency locking loop (O IL],) is shown in Fig. 2.

II. Mathematical Model

The transmission coefficient for a lossless FPE can be modeled as

$$T_{\mathrm{FPE}} = \frac{1}{1 + F \sin^2(\pi \frac{\nu}{\nu_{\mathrm{FSR}}})}, \tag{1}$$

where $F = (\frac{2}{\pi}\mathcal{F})^2$ is the coefficient of finesse, and ν_{FSR} is the free spectral range. The finesse $\mathcal{F}$ is given by

$$\mathcal{F} = \frac{\nu_{\mathrm{FSR}}}{\nu_{\mathrm{FWHM}}}, \tag{2}$$

where ν_{FWHM} is the fullwidth at half maximum of the FPE transmission peak. The frequency of the lasers, ν, is modeled as

$$\nu = \nu_{\mathrm{r}} + \nu_{\mathrm{e}} + \Delta\nu(t), \tag{3}$$

where ν_r is the resonance frequency, ν_e is the frequency deviation from the transmission peak, and $\Delta\nu(t)$ is the frequency modulat ion.

More specifically, the frequency modulation is modeled as

$$\Delta\nu(t) = \sqrt{2}\, g_m \cos(\Omega t), \tag{4}$$

where g_m is the modulation depth and Ω is the modulation frequency which is much higher than the inherent laser frequency jitter. In the following, the terms "modulation frequency" and "fundamental frequency" will be used interchangeably. Equation (1) is plotted in Fig. 3 for the custom, high finesse FPE used in laboratory development work. The cavity length of this FPE is 5 cm, which results in a free spectral range of 3 GHz. The full width at half maximum, ν_{FWHM}, is experimentally measured to be 300 KHz. These cavity parameters are used throughout this paper.

The output of the photodetector is modeled approximately as

$$v(t) = \sqrt{2}A\, T_{FPE}(\nu_e, t) + n(t), \tag{5}$$

where the noise $n(t)$ is modeled as a narrowband Gaussian random process. Using equat ion (1)-(5), the expression for the photodetector output can be approximated as

$$v(t) = \sqrt{2}A \frac{1}{1 + F \sin^2(\pi \frac{\nu_r + \nu_e + \sqrt{2} g_m \cos(\Omega t)}{\nu_{FSR}})} + n(t), \tag{6}$$

This model effectively assumes that the FPE reacts instantaneouly to changes in the modulation frequency, Ω. This assumption is reasonable if the modulation frequency of the drive oscillator is much less than ν_{FWHM}. (The finite response time tof the FPE is, however, taken into account in deriving the power spectral density of frequency jitter in Appendix A.)

Figures 4. shows the normalized photodetector output as the laser is modulated by the drive oscillator, Specifically, the output is plotted as a function of time for the case of

no frequency locking error and in the absence of noise. A similar plot is shown in Fig. 5 for the case when some frequency locking error is present. This frequency locking error is responsible for the appearance of a fundamental component (period 0.01 relative units) in Fig. 5.

III. Fourier Expansion and Optimal Modulation Depth

Note that the signal portion of the photodetector output, given by the first term of the right hand side of (6) , is periodic with period $T = \frac{2\pi}{\Omega}$. This periodicity suggests the existence of a Fourier series expansion for the signal. To extract the error information contained in each harmonic, the photodetector output signal is expanded as a trigonometric Fourier series:

$$v(t) = \sqrt{2}A\left\{a_0 + \sum_{n=1}^{\infty}\left[a_n \cos(n\Omega t) + b_n \sin(n\Omega t)\right]\right\} + n(t). \tag{7}$$

The Fourier coefficients are given by

$$a_0 = \frac{1}{T}\int_{t_0}^{t_0+T}\left[\frac{1}{1 \mp F\sin^2\left(\pi\frac{\nu_r + \nu_e + \sqrt{2}g_m\cos(\Omega t)}{\nu_{FSR}}\right)}\right]dt,$$

$$a_n = \frac{2}{T}\int_{t_0}^{t_0+T}\left[\frac{1}{1 + F\sin^2\left(\pi\frac{\nu_r + \nu_e + \sqrt{2}g_m\cos(\Omega t)}{\nu_{FSR}}\right)}\right]\cos(n\Omega t)\,dt, \quad \text{and}$$

$$b_n = \frac{2}{T}\int_{t_0}^{t_0+T}\left[\frac{1}{1 \mp F\sin^2\left(\pi\frac{\nu_r + \nu_e + \sqrt{2}g_m\cos(\Omega t)}{\nu_{FSR}}\right)}\right]\sin(n\Omega t)\,dt. \tag{8}$$

One may choose $t_0 = -2\pi/2$ so that the integration limits become symmetric and the b_n are thus seen to be identically zero.

Again, the OFLL's synchronous detector will pass only that portion of the photodetector output that matches its reference input (i.e. the drive oscillator) in both frequency and phase. The error signal can therefore be written as

$$e(t) = Aa_1(\nu_e, g_m) + \hat{n}(t), \tag{9}$$

where the fundamental Fourier coefficient depends on both frequency locking error, ν_e, and the choice of modulation depth, g_m. The $\hat{n}(t)$ is the equivalent noise process created by multiplying the noise at the photodetector output with the oscillator signal. The error signal $e(t)$ is then low-pass filtered and fed back to t he laser control inputs.

As an alternative to the Fourier series expansion, the photodetector output may be approximated by a first-order Taylor series expansion [5], This approach yields an error signal

$$e(t) \approx -8\, A \frac{\sqrt{2} g_m}{\nu_{F\ WHM}^2}\, \nu_e \text{ i“ } \hat{n}(t), \qquad (10)$$

promotional to ν_e. Hewer (10) is only valid for small g_m and is best viewed as a qualitative descript ion of the error signal.

It is, of course, desirable to maximize the error signal for a given laser-vs.-FPE frequency offset, The fundamental Fourier coefficient is plotted as a function of modulation depth in Fig. 6. Note that the error signal reaches a maximum at approximately 80 KHz, indicating the existence of an optimal modulation depth. For comparison, Fig. 6 also plots the first-order Taylor series expansion of the error signal,

Figure 7 shows the fundamental Fourier coefficient as a function of modulation depth for several values of frequency locking error. This figure confirms that the optimal modulation depth is $\approx$ 80 KHz and is fairly independent of frequency locking error. Figure 8 shows the fundamental Fourier coefficient as a function of frequency locking error for modulation depths of 70, 80 and 90 KHz. This figure indicates that the error signal amplitude is insensitive to small variation in modulation depth for frequency locking errors as large as ± 50 KHz.

IV. Frequency-Locked Operation and Effect of Loop Noise

A simplified block diagram of the OFLL is shown in Fig, 9, where $\nu_{JIT}(t)$ is the frequency jitter due to laser frequency noise, $\nu_e(t)$ is the frequency error, Z/$_c$(t) is the

frequency correction, $\hat{n}(t)$ is the additive noise, and A is proportional to the laser signs] power at the input of the FPE. The loop gain K is the product of the laser tuning coefficient and all other amplifier gains, and $F(s)$ is the loop filter transfer function. The function $g_{\mathrm{NL}}(\nu_e)$ is a nonlinear function of ν_e, and is the fundamental Fourier coefficient evaluated at the optimal modulation depth of 80 KHz. When the frequency locking error is small the nonlinear function $g_{\mathrm{NL}}(\nu_e)$ can be approximated as

$$g_{\mathrm{NL}}(\nu_e) \approx \dot{g}_{\mathrm{NL}}(0)\nu_e, \tag{11}$$

where $\dot{g}_{\mathrm{NL}}(0)$ is the derivative of $g_{\mathrm{NL}}(\nu_e)$ with respect to ν_e evaluated at $\nu_e = 0$. The exact and approximate forms of $g_{\mathrm{NL}}(\nu_e)$ are plotted in Fig. 10; this plot verifies that approximation (11) is accurate provided the frequency locking error is less than ± 30 KHz.

It can be shown that the OFLL closed loop transfer function, from $\nu_{\mathrm{JIT}}(t)$ to $\nu_c(t)$, is [6]

$$H_1(s) = \frac{A\dot{g}_{\mathrm{NL}}(0)KF(s)}{s + A\dot{g}_{\mathrm{NL}}(0)KF(s)}, \tag{12}$$

where F(s) is the loop filter transfer function. The transfer function from $\nu_{\mathrm{JIT}}(t)$ to $\nu_e(t)$, $H_2(s)$, is related to the closed loop transfer function by $H_2(s) = 1 - H_1$ (s),

The performance of the OFLL is affected by both additive noise and frequency noise, When the loop is operating in the linear region, the effects of individual noise sources can be determined separately and then combined to obtain the overall result [7], The variance in frequency offset due to additive noise can be written as

$$\sigma^2_{\mathrm{AN}} = \int_0^\infty |H_1(j2\pi f)|^2 \frac{S_{\mathrm{AN}}(f)}{(A\dot{g}_{\mathrm{NL}}(0))^2}\, df. \tag{13}$$

where $S_{\mathrm{AN}}(f)$ is the one sided power spectral density (PSD) of the additive noise [6, 7, 9]. The contribution due to frequency jitter can be calculated as

$$\sigma^2_{\mathrm{JIT}} = \int_0^\infty |H_2(j2\pi f)|^2 S_{\mathrm{JIT}}(f)\, df, \tag{14}$$

where $S_{\mathrm{JIT}}(f)$ is the PSD of the frequency jitter [6, 7, 9]. The PSD of the frequency jitter can be further expanded (Appendix A) as:

$$S_{\mathrm{JIT}}(f) = \left[\frac{\sin(\pi f \Delta t)}{(\pi f \Delta t)}\right]^2 \left[k_1 + \frac{k_2}{f} + \frac{k_3}{f^2}\right] \qquad 0 < f < \infty, \tag{15}$$

where At represents the photon lifetime of the FPE. The photon lifetime is related to the FPE's ν_{FWHM} by $\nu_{\mathrm{FWHM}} \approx 1/(\pi \Delta t)$.

For a suitable choice of $F(s), H_2(j2\pi f)$ will have zeros at $f =$ O, characteristic of a perfect second-order loop [6, 7]. This loop will then be unconditionally stable and the zeros of $H_2(j2\pi f)$ at $f =$ O will compensate for the poles of the frequency jitter spectrum, allowing the loop to accurately track low frequency fluctuations, Moreover, a perfect linearized second-order loop will also have a theoretically infinite pull-in range for frequency acquisition [6], For these reasons, $F(s)$ is chosen to be of the form

$$F(s) = \frac{1 + \tau_2 s}{\tau_1 s}. \tag{16}$$

For a perfect second-order OFLL, the damping factor, ζ, and one sided loop bandwidth, B_{L}, are given by [7]

$$\zeta \triangleq \frac{1}{2}\sqrt{\frac{\tau_2^2 A \dot{g}_{\mathrm{NL}}(0) K}{\tau_1}}, \tag{17}$$

and

$$\begin{aligned} B_{\mathrm{L}} &\triangleq \int_0^\infty |H_1(j2\pi f)|^2 \, df \\ &= \frac{\tau_1 + \tau_2^2 A \dot{g}_{\mathrm{NL}}(0) K}{4\tau_1 \tau_2} \end{aligned} \tag{18}$$

respect ivel y.

When the additive noise is dominated by shot noise with one sided power spectral density No [Watts/Hz], then the variance due to additive noise becomes

$$\sigma_{\mathrm{AN}}^2 = \frac{1}{\rho \dot{g}_{\mathrm{NL}}^2(0)} B_{\mathrm{L}} \ , \tag{19}$$

where $\rho = \frac{A^2}{N_0}$. The contribution of frequency jitter to the variance can be written, using (15) as

$$\sigma^2_{\mathrm{JIT}} = \int_0^\infty |H_2(j2\pi f)|^2 \left[\frac{\sin(\pi f \Delta t)}{(\pi f \Delta t)}\right]^2 \left[k_1 + \frac{k_2}{f} + \frac{k_3}{f^2}\right] df$$
$$= \sigma^2_{\mathrm{w}} + \sigma^2_{1/f} + \sigma^2_{1/f^2}, \qquad (20)$$

where σ^2_{w}, $\sigma^2_{1/f}$, and σ^2_{1/f^2} are the contributions of the white, $1/f$, and $1/f^2$ components of the frequency noise.

For a general perfect OFLL, the above integrals for σ^2_{w}, $\sigma^2_{1/f}$, and σ^2_{1/f^2} are very difficult to evaluate analytically. However, some simplifications can be made if the OFLL is assumed to be critically damped, i.e. $\zeta = 1$. Detailed calculations of these $\zeta = 1$ integrals for each of the frequency noise contributions are given in Appendices B, C, and D. The results are summarized below, where $B_{\mathrm{L}} = 5/(4\tau_2)$ for a critically-damped, perfect second-order OFLL.

The white frequency noise contribution is calculated in Appendix B:

$$\sigma^2_{\mathrm{w}} = \frac{5}{32}\frac{1}{(B_{\mathrm{L}}\Delta t)}\frac{k_1}{\Delta t}\left\{1 - \left[1 + \frac{8}{5}B_{\mathrm{L}}\Delta t\right]\exp\left(-\frac{8}{5}B_{\mathrm{L}}\Delta t\right)\right\}. \qquad (21)$$

When $B_L\Delta t \ll 1$, (21) can be approximated by

$$\sigma^2_{\mathrm{w}} \approx \frac{1}{2}\frac{k_1}{\Delta t} \qquad (B_{\mathrm{L}}\Delta t \ll 1). \qquad (22)$$

When $B_L\Delta t \gg 1$, then $\exp\left(-\frac{8}{5}B_{\mathrm{L}}\Delta t\right) \approx 0$, and (21) can be reduced to

$$\sigma^2_{\mathrm{w}} \approx \frac{5}{32}\frac{1}{(B_{\mathrm{L}}\Delta t)}\frac{k_1}{\Delta t} \qquad (B_{\mathrm{L}}\Delta t \gg 1). \qquad (23)$$

The contribution of the $1/f$ component can not be calculated in a closed form. However it is calculated in terms of exponential integrals in Appendix C as

$$\sigma^2_{1/f} = \frac{5}{16}\frac{k_2}{(B_{\mathrm{L}}\Delta t)}\left\{\mathrm{E}_1\left(\frac{8}{5}B_{\mathrm{L}}\Delta t\right)\exp\left(\frac{8}{5}B_{\mathrm{L}}\Delta t\right) + \mathrm{Ei}\left(\frac{8}{5}B_{\mathrm{L}}\Delta t\right)\exp\left(-\frac{8}{5}B_{\mathrm{L}}\Delta t\right)\right\}, \qquad (24)$$

where El(z), and Ei(x) are known as exponential integrals given by [12],

$$E_1(z) = \int_x^\infty \frac{e^{-t}}{t}\,dt \qquad (|\arg z| < \pi), \qquad \text{and}$$

$$Ei(x) = -\frac{1}{2}\left[E_1(-x + i\infty) + E_1(-x - i\infty)\right]. \tag{25}$$

Equation (24) may be approximated for extreme values of $B_L\Delta t$ to obtain some physical insight.

When $B_L\Delta t$ <<1, the approximate expression for (24) can be obtained, using series expansion of El(z), as

$$\sigma^2_{1/f} \approx k_2\left[1 - \gamma - \ln\left(\frac{8}{5}B_L\Delta t\right)\right] \qquad (B_L\Delta t << 1), \tag{26}$$

where $\gamma = 0.577\ldots$ is Euler's constant, (hi the other hand, when $B_L\Delta t$ >> 1, (24) can be approximated using the asymptotic expansion of El(z) as

$$\sigma^2_{1/f} \approx \frac{25}{64}\frac{k_2}{(B_L\Delta t)^2} \qquad (B_L\Delta t >> 1). \tag{27}$$

The contribution of the 1 $/f^2$ frequency noise component is calculated in Appendix D *as*

$$\sigma^2_{1/f^2} = \frac{125}{512}\frac{\pi^2}{((B_L\Delta t)^2 B_L}\frac{k_3}{B_L}\left\{1 - \left[1 + \frac{8}{5}B_L\Delta t\right]\exp\left(-\frac{8}{5}B_L\Delta t\right)\right\}. \tag{28}$$

When $B_L\Delta t$ <<1, *(28)* can be approximately written as

$$\sigma^2_{1/f^2} \approx \frac{5\pi^2}{16}\frac{k_3}{B_L} \qquad (B_L\Delta t << 1). \tag{29}$$

When $B_L\Delta t >> 1$, then (28) can be reduced to

$$\sigma^2_{1/f^2} \approx \frac{125}{512}\frac{\pi^2}{(B_L\Delta t)^2}\frac{k_3}{B_L} \qquad (B_L\Delta t >> 1). \tag{30}$$

Figure 11 shows the contributions of σ_w^2, $\sigma_{1/f}^2$, and σ_{1/f^2}^2. Also shown is the sum of these contributions, σ_{JIT}^2. This figure is plotted for At =1.06 microseconds, k_1= 0.1 Hz, k_2= 0.'75 x 10^4 Hz^2, and k_3= 0.5 x 10^7 Hz^3 as experimentally measured in [S].

Because the additive noise and the frequency jitter arc independent, the total frequency locking error variance can be written as

$$\begin{aligned}\sigma_{\nu_e}^2 &= \sigma_{AN}^2 + \sigma_{JIT}^2 \\ &= \frac{1}{\rho \dot{g}_{NL}^2(0)} B_L \\ &+ \frac{5}{32}\frac{k_0}{(B_L\Delta t)^2}\Delta t\left\{1 - \left[1 - \frac{8}{5}B_L\Delta t\right]\exp\left(-\frac{8}{5}B_L\Delta t\right)\right\} \\ &+ \frac{5}{16}\frac{k_1}{(B_L\Delta t)}\left\{E_1\left(\frac{8}{5}B_L\Delta t\right)\exp\left(\frac{8}{5}B_L\Delta t\right) + \mathrm{Ei}\left(\frac{8}{5}B_L\Delta t\right)\exp\left(-\frac{8}{5}B_L\Delta t\right)\right\} \\ &+ \frac{125}{512}\frac{\pi^2 k_2}{(B_L\Delta t)^2 B_L} - \left[1 + \frac{8}{5}B_L\Delta t\right]\exp\left(-\frac{8}{5}B_L\Delta t\right)\Big\}. \end{aligned} \quad (31)$$

When $B_L\Delta t$ <<1, (31) can be approximately written using (22) , (26) , and (29) as

$$\sigma_{\nu_e}^2 \approx \frac{1}{\rho \dot{g}_{NL}^2(0)} B_L + \frac{1}{2}\frac{d}{\Delta t} + k_1\left[-\gamma - \ln\left(\frac{8}{5}B_L\Delta t\right)\right] + \frac{5\pi^2}{16}\frac{k_3}{B_L} \qquad (B_L\Delta t << 1). \quad (32)$$

On the other hand, when $B_L\Delta t$ >> 1, (31) can be approximated using (23) , (27) , and (30) as

$$\sigma_{\nu_e}^2 \approx \frac{1}{\rho \dot{g}_{NL}^2(0)} B_L + \frac{5}{32}\frac{1}{(B_L\Delta t)}\frac{k_1}{\Delta t} + \frac{25}{64}\frac{k_1}{(B_L\Delta t)^2} + \frac{125}{512}\frac{\pi^2}{(B_L\Delta t)^2}\frac{k_3}{B_L} \qquad (B_L\Delta t >> 1). \quad (33)$$

Figure 12 plots the variances due to additive noise and frequency jitter, as well as their sum. The additive noise plot assumes ρ = 90 dB-Hz. It can be seen from Fig. 12 that performance of the OFLL is frequency noise limited if the loop bandwidth is. less than ≈ *2300* Hz and otherwise shot noise limited. A family of curves representing total rms frequency locking error for different values of *p* is plotted in Fig, 13 as a function of loop bandwidth. Figure 13 shows that an rms frequency locking error of less than 600 Hz can

be achieved with a loop bandwidth of 500 Hz for p greater than 80 dB. The fact that this locking error is much less than 30 KHz indicates that the linear approximation (11) is self-consistent,

Fig. 13 also indicates the existence of an optimal loop bandwidth resulting in a minimum frequenc y locking error variance. This optimal bandwidth depends on ρ and is about 500 Hz for ρ between 80 dB and 100 dB. The optimal loop bandwidth of an OFLL can be calculated for any given ρ.

V. Summary and Conclusions

A basic laser frequency locking system employing a Fabry-Perot et alon and frequency modulating oscillator was outlined. A theoretical analysis of this optical frequency locking loop (OFLL) estimated its performance in the presence of shot noise and frequency noise typical of diode-pumped Nd:YAG lasers. In paticular:

a) Contributions from shot noise and each of the frequency noise components to total frequency locking error were analyzed and displayed as a function of loop bandwidth.

b) An optimal modulation depth, g_m, of $\approx$ 80 KHz that maximized the error signal amplitude and minimized frequency locking error was identified.

c) 'l'he expected performance of the OFLL, as measured by $\sigma^2_{\nu_e}$ was then estimated for this choice of optimal modulation depth.

The analysis shows that an rrns frequency locking error, i.e. an offset of laser-vs.-FPE transmission peak frequency, of less than 600 Hz can be achieved with a loop bandwidth of 500 Hz for ρ greater than 80 dB. This verifies that the linear approximation (11) is self-consistent for analyzing the proposed frequency locking subsystem using FPE. Based on this analysis, an optimum loop bandwidth which minimizes frequency locking error can be determined for a given ρ.

VII. Acknowledgments

The author would like to thank Dr. Eldred Tubbs, Dr. Serge Dubovitsky ant] Dr. Yekta Gursel of Jet Propulsion Laboratory, and Professor Robert A, Scholt z of University of Southern California for their valuable discussions. The research described in this paper was carried out by the Jet Propulsion Laboratory, California Institute of Technology, under contract with the National Aeronautics and Space Administration.

APPENDIX A: CALCULATION OF THE FREQUENCY JITTER PSD

The frequency noise process, $f_N(t)$, is modeled to cent ain a white component, a $1/f$ component, and a $1/f^2$ component. Mathematically, the PSD of frequency noise is modeled as

$$S_{FN}(f) = k_1 + \frac{k_2}{f} + \frac{k_3}{f^2} \qquad 0 < f < \infty, \tag{Al}$$

where k_1 [Hz] is the one sided PSD of the white component, The constants $k_2[\mathrm{Hz}^2]$ and $k_3[\mathrm{Hz}^3]$ indicate the magnitudes of the $1/f$ and $1/f^2$ components of the frequency noise respectively. The frequency noise model given in (Al) was verified experimentally in [8] and indirectly in [9, 10]. The parameters associated with the frequency noise of the a diode-pumped Nd:YAG ring laser were determined to be $k_1 = 0.1$ Hz, $k_2 = 0.75 \times 10^4 \mathrm{Hz}^2$, and $k_3 = 0{,}5 \times 10^7 \mathrm{Hz}^3$ [8].

High frequency content of the frequency noise is limited by the fact the finite response t ime of the FPE. The detected frequency jitter can be related to the frequency noise by the following model as

$$\nu_{JIT}(t) = \frac{1}{\Delta t} \int_{t-\Delta t}^{t} f_N(\tau)\, d\tau, \tag{A2}$$

where At is represents the photon lifetime of the FPE. The photon lifetime is related to the FPE's ν_{FWHM} by $\nu_{FWHM} \approx 1/(\pi \Delta t)$

Equation (A2) is a convolution of the frequency noise with a time window of height 1 /At, and width Δt. Mathematically

$$\nu_{JIT}(t) = \int_{-\infty}^{+\infty} f_N(\tau) c(t-\tau)\, d\tau = f_N(t) * \; c(t), \tag{A3}$$

where

$$c(t) = \begin{cases} 1 \text{ if } 0 < t < \mathrm{A}t \\ O \text{ otherwise.} \end{cases} \tag{A4}$$

By using the fundamental theorem of the power spectrum [13], the PSD of the frequency

jitter becomes

$$S_{JIT}(f) = \left[\frac{\sin(\pi f \Delta t)}{(\pi f \Delta t)}\right]^2 S_{FN}(f)$$

$$= \left[\frac{\sin(\pi f \Delta t)}{(\pi f \Delta t)}\right]^2 \left[k_1 + \frac{k_2}{f} + \frac{k_3}{f^2}\right] \qquad 0 < f < \infty. \qquad (A5)$$

APPENDIX B: CALCULATION OF WHITE FREQUENCY NOISE CONTRIBUTION

The frequency locking error variance due to white frequency noise for a critically-damped, perfect sec.ond-order OFLL can be written as

$$\sigma_w^2 = k_1 \int_0^\infty \left| \frac{\alpha^2 f^2}{4 + \alpha^2 f^2} \right|^2 \left[\%\%' 1^{2\prime\prime} \right] \qquad (B1)$$

where $\alpha = 5\pi/(2B_L)$. This can be rewritten as

$$\sigma_w^2 = \frac{1}{2} \frac{k_1}{(\pi \Delta t)^2} \left\{ \int_0^\infty \frac{f^2}{\left[\left(\frac{2}{\alpha}\right)^2 + f^2 \right]^2} df - \int_0^\infty \frac{f^2}{\left[\left(\frac{2}{\alpha}\right)^2 + f^2 \right]^2} \cos(2\pi f \Delta t)\, df \right\}. \qquad (B2)$$

Using 3.253 and 3.733.3 of [11], along with L'Hôpitol's rule of calculus, (B2) reduces to

$$\sigma_w^2 = \frac{5}{32} \frac{1}{(B_L \Delta t)} \frac{k_1}{\Delta t} \left\{ 1 - \left[1 - \frac{8}{5} B_L \Delta t \right] \exp\left(-\frac{8}{5} B_L \Delta t \right) \right\}. \qquad (B3)$$

When $B_L \Delta t << 1$, then (B3) can be approximated by truncating the Taylor series expansion of $\exp(-\frac{8}{5} B_L \Delta t)$ as

$$\sigma_w^2 \approx \frac{1}{2} \frac{k_1}{\Delta t} \qquad (B_L \Delta t << 1). \qquad (B4)$$

When $B_L \Delta t >> 1$, then $\exp\left(-\frac{8}{5} B_L \Delta t\right) \approx 0$, and (B3) can be reduced to

$$\sigma_w^2 \approx \frac{5}{32} \frac{1}{(B_L \Delta t)} \frac{k_1}{\Delta t} \qquad (B_L \Delta t >> 1). \qquad (B5)$$

APPENDIX C: CALCULATION OF $1/f$ FREQUENCY NOISE CONTRIBUTION

The frequency locking error variance due to $1/f$ frequency noise for a critically-damped, perfect second-order OFLL can be written as

$$\sigma_{1/f}^2 = k_2 \int_0^\infty \left| \frac{\alpha^2 f^2}{4 + \alpha^2 f^2} \right|^2 \left[\frac{\sin(\pi f \Delta t)}{(\pi f \Delta t)} \right]^2 \frac{1}{f}\, df, \tag{C1}$$

$$= \frac{k_2}{(\pi \Delta t)^2} \int_0^\infty \frac{f}{\left[\left(\frac{2}{\alpha}\right)^2 + f^2 \right]^2} \sin^2(\pi f \Delta t)\, df. \tag{C2}$$

Noting that $\frac{f}{\left[\left(\frac{2}{\alpha}\right)^2 + f^2\right]^2} = -\frac{1}{2}\frac{d}{df}\frac{1}{\left[\left(\frac{2}{\alpha}\right)^2 + f^2\right]}$ and using integration by parts, (C2) can be reduced to

$$\sigma_{1/f}^2 = \frac{k_2}{(2\pi \Delta t)} \int_0^\infty \frac{1}{\left[\left(\frac{2}{\alpha}\right)^2 + f^2 \right]^2} [\sin(2\pi f \Delta t)]\, df. \tag{C3}$$

Using 3,723.1 of [11], (C3) is evaluated as

$$\sigma_{1/f}^2 = \frac{5}{16} \frac{k_1}{(B_L \Delta t)} \left\{ \mathrm{E}_1\left(\frac{8}{5} B_L \Delta t\right) \exp\left(\frac{8}{5} B_L \Delta t\right) + \mathrm{Ei}\left(\frac{8}{5} B_L \Delta t\right) \exp\left(-\frac{8}{5} B_L \Delta t\right) \right\}, \tag{C4}$$

where El(z) and $\mathrm{Ei}(x)$ arc known as exponential integrals and are given by [12],

$$\mathrm{E}_1(z) = \int_z^\infty \frac{e^{-t}}{t}\, dt \qquad (|\arg z| < \pi), \qquad \text{and} \tag{C5}$$

$$\mathrm{Ei}(x) = -\frac{1}{2}[\mathrm{E}_1(-x + i\infty) + \mathrm{E}_1(-x - \mathrm{ice})] \qquad (x > 0). \tag{C6}$$

More insight into $\sigma_{1/f}^2$ may be obtained by approximating (C4) for the two extreme cases of 13,, $\Delta t << 1$ and $B_L \Delta t >> 1$.

When the arguments of El (z) and $\mathrm{Ei}(x)$ are very small, they can be approximated by truncating their series expansion [12]:

$$\mathrm{E}_1(z) = -\gamma - \ln z - \sum_{n=1}^{\infty} \frac{(-1)^n z^n}{n n!} \qquad (|\arg z| < \pi)$$

$$\approx -\gamma - \ln z + z - \frac{1}{4} z^2, \qquad \text{and} \tag{C7}$$

$$\mathrm{Ei}(x) = \gamma + \ln x + \sum_{n=1}^{\infty} \frac{x^n}{n n!} \qquad (x > 0)$$

$$\approx \gamma + \ln x + x + \frac{1}{4} x^2 \tag{C8}$$

Therefore, for x <<1

$$[\mathrm{E}_1(x)\exp(x) + \mathrm{Ei}(x)\exp(-x)] \approx 2x(1 - \gamma - \ln x). \qquad (C9)$$

Using (C9), the expression for the variance due to 1/~ frequency noise simplifies to

$$\sigma_{1/f}^2 \approx k_1 \left[1 - \gamma - \ln(\frac{8}{5} B_L \Delta t)\right] \qquad (B_L \Delta t << 1). \qquad (c'1o)$$

When the arguments of El (z) and $\mathrm{Ei}(x)$ are large, they can be approximated by truncating their asymptotic expansions [12], as

$$\mathrm{E}_1(z) = \frac{e^{-z}}{z}\left\{1 - \frac{1}{2} + \frac{2}{z^2} - \frac{6}{z^3} + \ldots\right\} \qquad (|\arg z| < \frac{3}{2}\pi)$$

$$\approx \frac{e^{-z}}{z}\left\{1 - \frac{1}{zz} + \frac{2}{z^2}\right\}, \quad \text{and} \qquad (C11)$$

$$\mathrm{Ei}(x) = \sim^{r}\text{-}\left\{1 + \frac{1}{x} + \frac{2}{x^2} + \frac{6}{x^3} + \ldots\right\} \qquad (x > o)$$

$$\approx \frac{e^x}{x}\left\{1 + \frac{1}{x} + \frac{2}{x^2}\right\}. \qquad (C12)$$

Therefore, for x >>1

$$[\mathrm{E}_1(x)\exp(x) + \mathrm{Ei}(x)\exp(-x)] \approx \frac{2}{x}\left(1 + \frac{2}{x^2}\right). \qquad (C13)$$

Using (C13), the expression for the variance due to $1/f$ frequency noise now simplifies to

$$\sigma_{1/f}^2 \approx \frac{25}{64}\frac{k_1}{(B_L \Delta t)^2} \qquad (B_L \Delta t >> 1). \qquad (C14)$$

APPENDIX D: CALCULATION OF $1/f^2$ FREQUENCY NOISE CONTRIBUTION

The frequency locking error variance due to $1/f^2$ frequency noise for a critically-damped perfect second- order OFLL can bc writ ten as

$$\sigma^2_{1/f^2} = k_3 \int_0^\infty \left| \frac{\alpha^2 f^2}{4 + \alpha^2 f^2} \right|^2 \left[\frac{\sin(\pi f \Delta t)}{(\pi f \Delta t)} \right]^2 \frac{1}{f^2}\, df. \qquad (D1)$$

This can be rewritten as

$$\sigma^2_{1/f^2} = \frac{1}{2} \frac{k_3}{(\pi \Delta t)^2} \left\{ \int_0^\infty \frac{1}{\left[\left(\frac{2}{\alpha}\right)^2 + f^2 \right]^2} df - \int_0^\infty \frac{1}{\left[\left(\frac{2}{\alpha}\right)^2 + f^2 \right]^2} \cos(2\pi f \Delta t)\, df \right\}. \qquad (D2)$$

Using 3.251.4, and 3.729.1 of [11], (D2) reduces to

$$\sigma^2_{1/f^2} = \frac{125}{512} \frac{\pi^2}{(B_L \Delta t)^2} \frac{k_3}{B_L} \left\{ 1 - \left[1 + \frac{8}{5} B_L \Delta t \right] \exp\left(-\frac{8}{5} B_L \Delta t \right) \right\}. \qquad (D3)$$

When $B_L \Delta t << 1$, then (D3) can be approximated by truncating the Taylor series expansion of exp $(-\frac{8}{5} B_L \Delta t)$ as

$$\sigma^2_{1/f^2} \approx \frac{5\pi^2}{16} \frac{k_3}{B_L} \qquad (B_L \Delta t << 1). \qquad (D4)$$

When $B_L \Delta t >> 1$, then exp $(-\frac{8}{5} B_L \Delta t) \approx$ O, and (D3) can be reduced to

$$\sigma^2_{1/f^2} \approx \frac{125}{512} \frac{\pi^2}{(B_L \Delta t)^2} \frac{k3}{B_L} \qquad (B_L \Delta t >> 1). \qquad (D5)$$

REFERENCES

[1] C.-C. Chen, and M. Z. Win, "Laser Frequency Stability requirements for Coherent Space Communications," *Proc. of 45th Annual Symposium on Frequency Control*, pp. 500-507, Los Angeles, CA, May, 199].

[2] M. Z. Win, C.-C. Chen and R. A. Scholtz, "Optical Phase-Locked Loop (OPLL) for An Amplitude Modulated Communications Link Using Solid State Lasers," Submitted for publication in *IEEE Trans. Selected Area Commun.,* First Quarter, 1995.

[3] N. Nerheim, "Conceptual Design of a Dual-Wave Heterodyne Interferometer: Part 1, Design of a Single-Wave Heterodyne Interferometer," *JPL Engineering Memorandum, 343-1194,* August, 1990.

[4] N. Nerheim, "Conceptual Design of a Dual-Wave Heterodyne Interferometer: Part II. Design of a Double Heterodyne Interferometer," *JPL* Engineering *Memorandum, 343-1201,* September, 1990,

[5] S. Duvovitsky, "Proof-of- Concept Demonstration of Frequency Locking of Tunable Laser to a Fabry-Perot Etalon," *JPL Engineering Memorandum, 343-EM-1270,* July 9, 1992.

[6] A. J. Viterbi, *Principles of Coherent Communications, New* York :McGraw-Hill, Inc., 1962.

[7] W. C. Lindsey, *Synchronization Systems* in *Communication and Control,* Englewood Cliffs, NJ: Prentice-Hall, Inc., 1972.

[8] C.-C. Chen and M. Z. Win, "Frequency Noise Measurement of Diode-Pumped Nd:YAG Ring Lasers," *IEEE Photonics Technology Lett.*, vol. *2,* no. 11, pp. 772-774, Nov., *1990.*

[9] M. Z. Win, C.-C. Chen and R. A. Scholtz, "Optical Phase-Locked Loop (OPLL) for Free-Space Laser Communications with Heterodyne Detection," *Proc. SPIE, Frcc-*

Space Laser Communication Technologies III, vol. 1417, Jan., 1991.

[10] M. Z. Win, C.-C. Chen and R. A. Scholtz, "Analysis of Noise in Optical Phase-Locked Loop (OPLL)," *NASA Tech. Briefs*, Sept. 1993.

[11] I. S. Gradshteyn, and I. M. Ryzhik, *Tables of Integrals, Series, and Products, Corrected and Enlarged Edition,* Orlando, Fl., Academic Press, Inc., 1980, p. 67, section 2.161.

[12] M. Abramowitz, and I. E. Stegun, *Handbook of Mathematical Functions,* Goverment Printing Office, 1970, pp. 228, section 5.1.

[13] A. Papoulis, *Probability, Random Variables, and Stochastic Processes,* New York: McGraw-Hill, Inc., 1965.

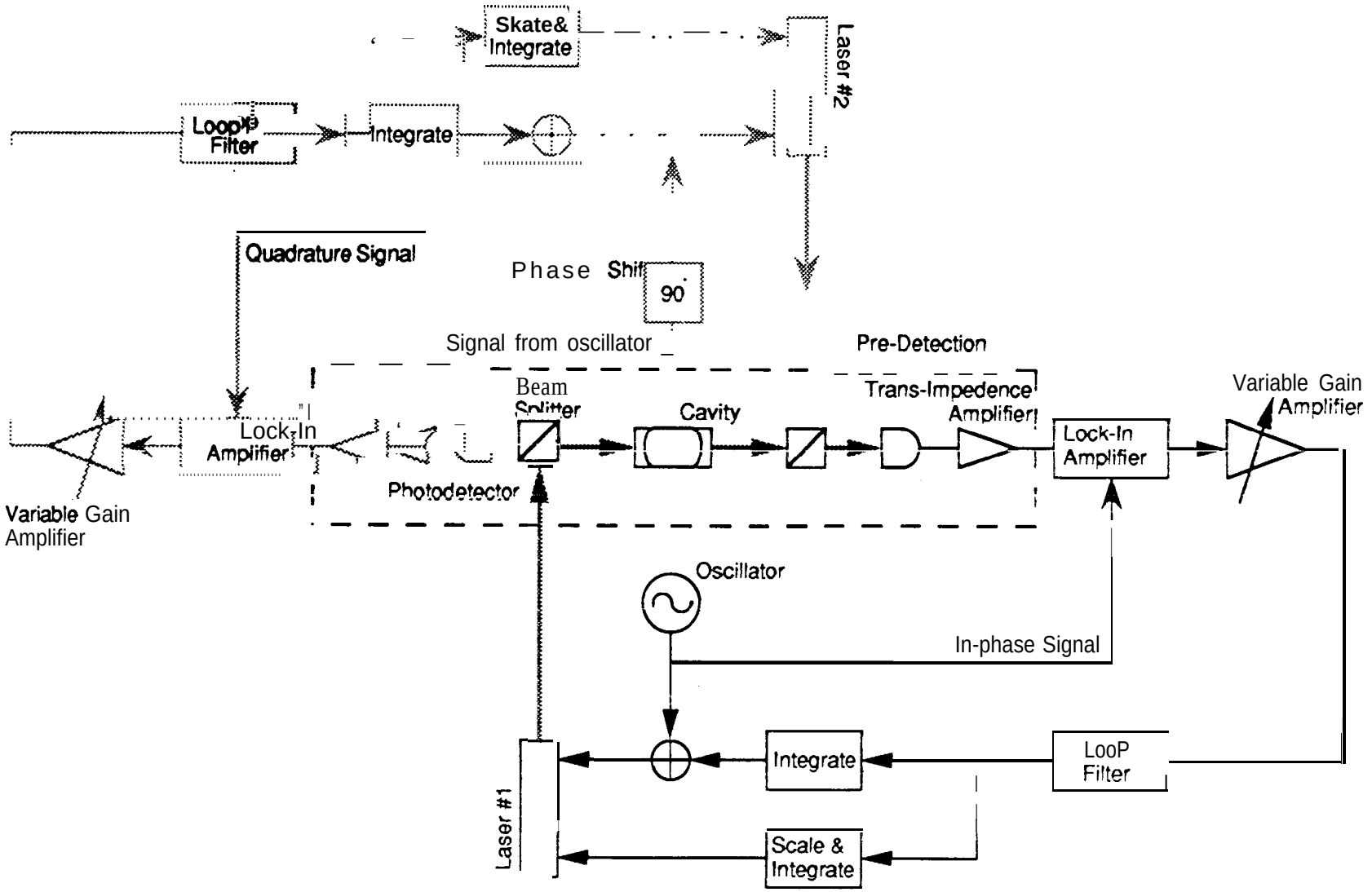

Figure 1. The conceptual diagram of frequency stabilization subsystem using Fabry-Perot Etalon and **dithering** oscillator. Only the optical path of the laser #1 is shown.

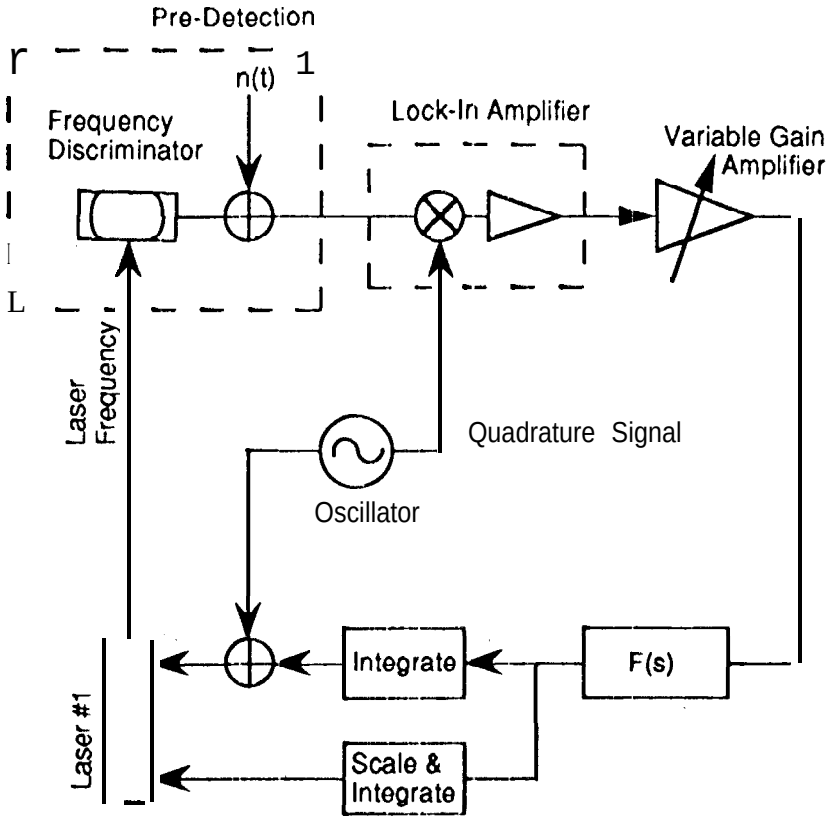

Figure 2. Basic elements of a frequency stabilization subsystem.

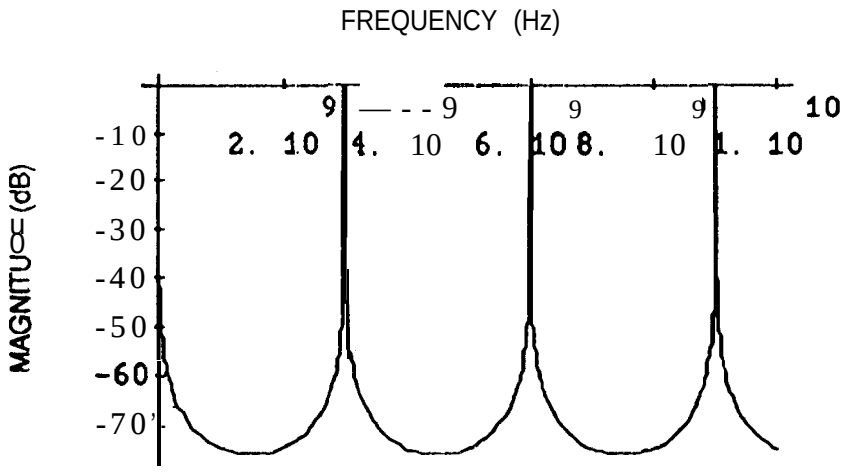

Figure 3. Frequency response of the custom high finesse Fabry-Perot Etalon. The cavity length is 5 cm, which results in a free spectral range of 3 GHz. Fullwidth at half maximum is experimentally measured to be 300 KHz,

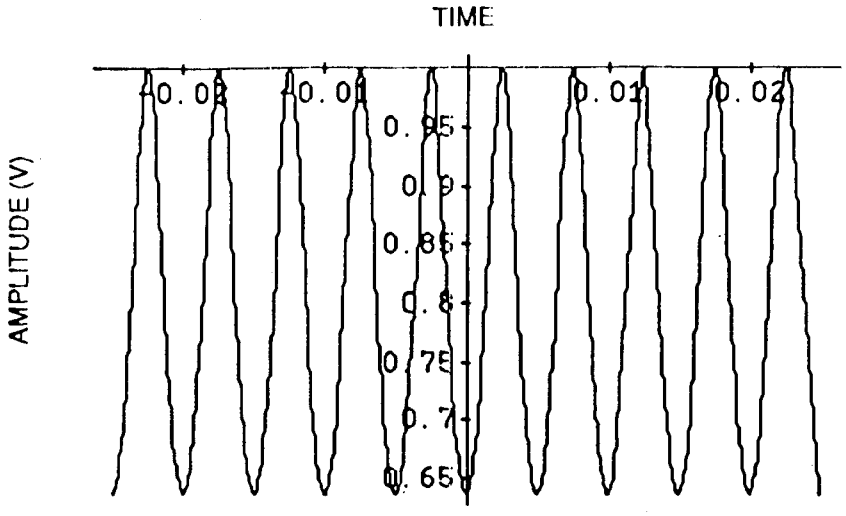

Figure 4. Normalized photodetector output as the laser is modulated by quadrature dithering oscillator: no frequency locking error and zero noise.

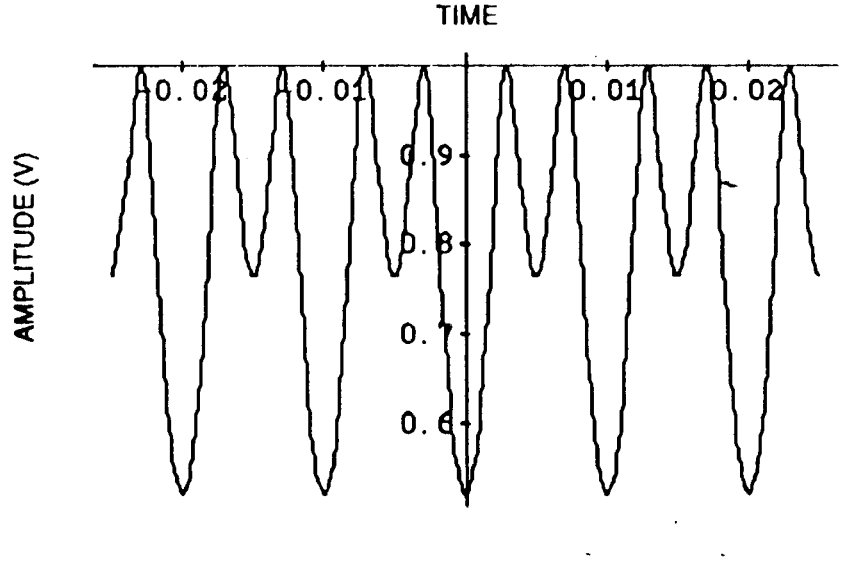

Figure 5. Normalized photodetector output as the laser is modulated by quadrature dithering oscillator: small frequency locking error and zero noise.

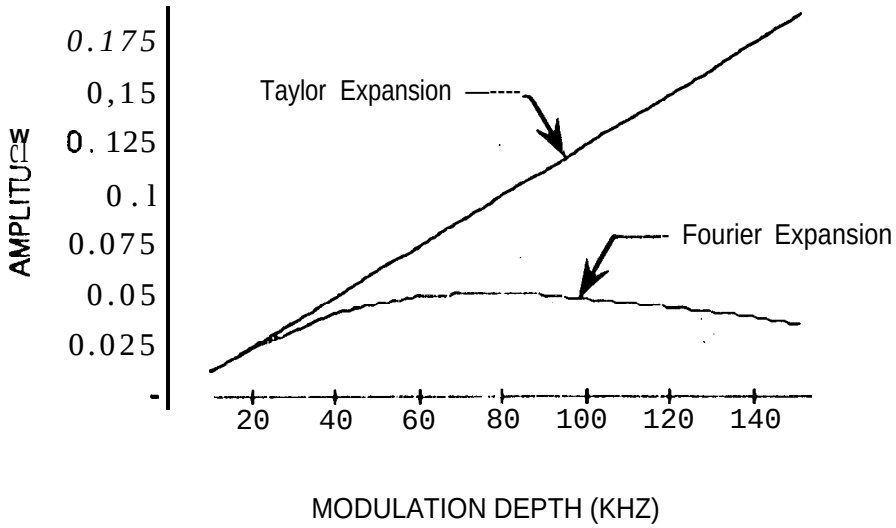

Figure 6. Fundamental Fourier coefficient as a function of modulation depth for some frequency locking error. Also shown is a first-order Taylor series expansion, valid for small modulation depth.

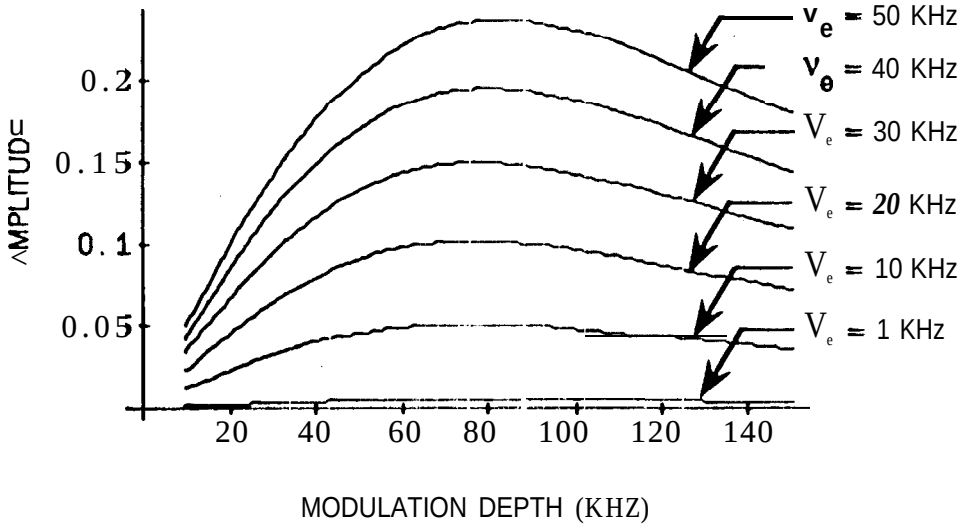

Figure 7. Fundamental Fourier coefficient as a function of modulation depth for several values of frequency locking error.

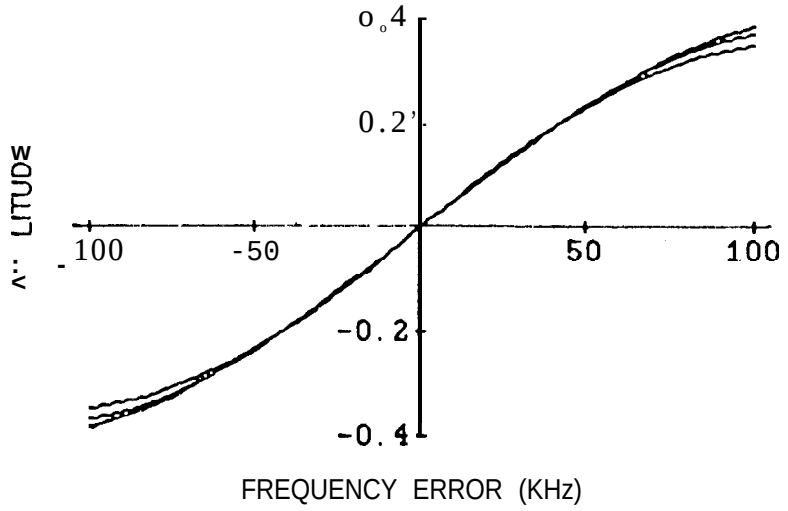

Figure 8. Frequency locking error signal as a function of frequency locking error at optimal modulation depth of 80 KHz. Also shown are the curves for modulation depths of 70 KHz and 90 KHz.

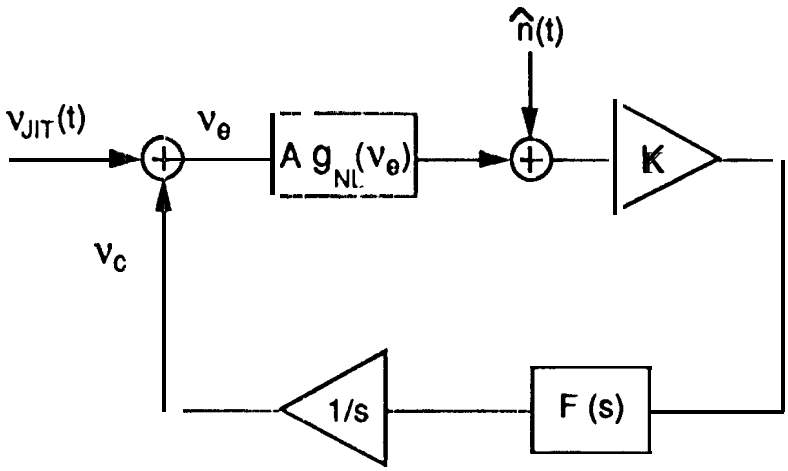

Figure 9. A simplified block diagram of the optical frequency locking loop (OFLL).

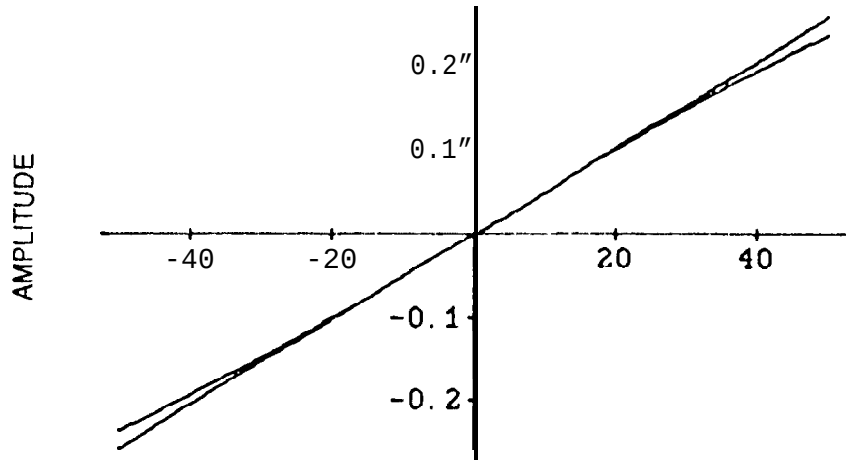

Figure 10. Linear approximation and exact value of $g_{NL}(\nu_e)$ as a function of frequency locking error at optimal modulation depth of 80 KHz.

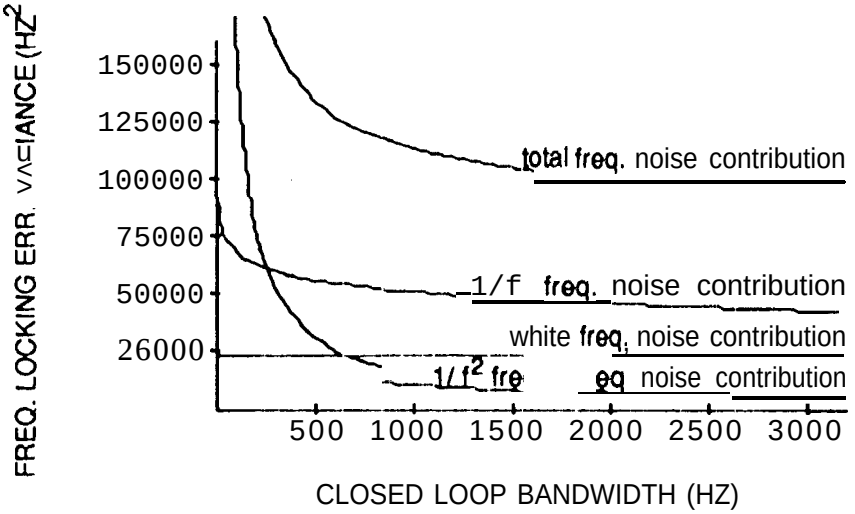

Figure 11. Contributions of white, I/f, and 1 /f² frequency noise components to the frequency locking error as a function of loop bandwidth. Also shown is the sum of these contributions.

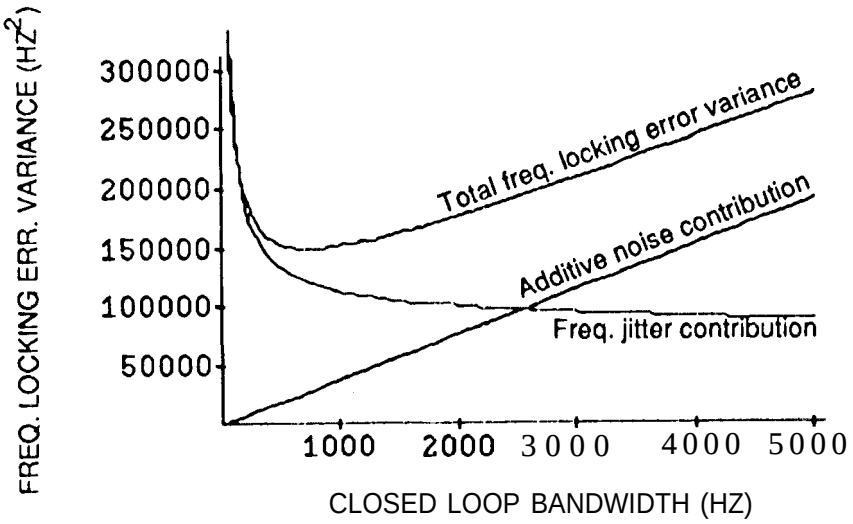

Figure 12. Contributions of frequency jitter and additive noise to the frequency locking error. Also shown is the sum of these contribution. This figure is plotted for p = 90 dB-Hz.

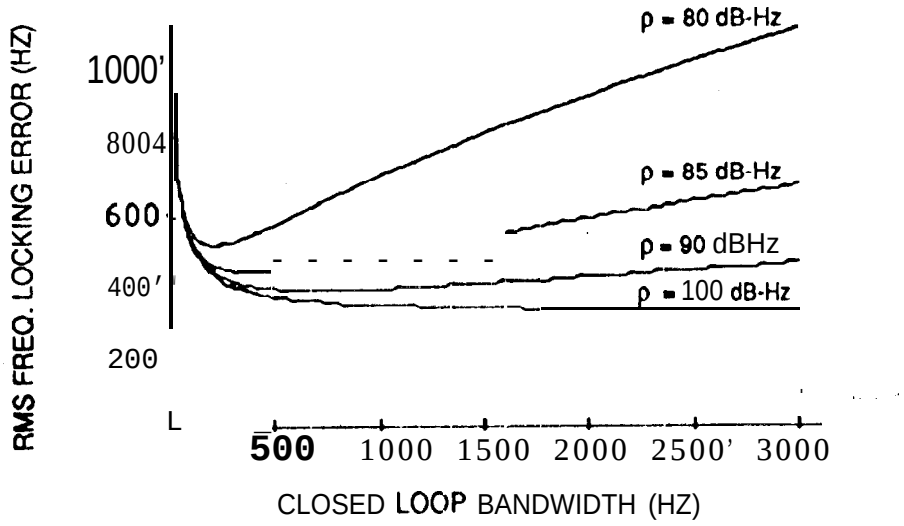

Figure 13. Root mean squared frequency locking error as a function of loop bandwidth for several values of p.